Revenue maximisation through model predictive control

Effect of draining efficiency on energy storage and revenues

By

Sander Bakker
s3331814

A thesis submitted to
the University of Groningen
for the degree of
BACHELOR OF SCIENCE

Ocean Grazer
prof. dr. ir. Bayu Jayawardhana & ir. Mehran Mohebbi
Faculty of Science and Engineering
University of Groningen
June 2020

ABSTRACT

Model predictive control is used for revenue maximisation in a network of Ocean Batteries. If efficiency is assumed to be high, the model intuitively decides on energy storing and draining operations. This model was however built on assumptions simplifying its behaviour. Efficiency has proven to vary during draining operations, from literature and has been quantified with previous research on the Ocean Grazer. This study investigates the validity of the current model and subsequently, the model will be complemented with this varying efficiency. This altered behaviour of the model after implementation will be analysed and discussed. Every turbine has a different 'efficiency curve' which plots the efficiency against the dimensionless flow-rate, *i.e.* with respect to its best efficiency point. In the conceptual Ocean Grazer set-up, which serves as a basis to this research, the use of a pump running as turbine is proposed. The model is generalised in such a way that simulations can be done both with standalone as well as pumps running as turbines.

Table of Contents

List of Figures

List of Tables

List of Acronyms

BEP Best Efficiency Point 7, 13

BSP Balance Service Provider 11

CFD Computational Fluid Dynamics 14, 22, 34

CTO Chief Technology Officer 3, 4

FRR Frequency Restoration Reserves 10, 11, 22

MPC Model Predictive Control 2, 10, 12, 13, 16, 19, 21, 25, 26, 28, 29, 34, 53

OB Ocean Battery 1, 3, 5, 6, 7, 8, 9, 10, 11, 12, 14, 17, 19, 20, 22, 23, 24, 25, 26, 27, 28, 29, 31, 32, 34

OG Ocean Grazer 1, 3, 4, 10, 11, 19, 23, 26, 32, 33, 34, 53

PAT Pump as Turbine 1, 2, 7, 8, 9, 13, 15, 18, 19, 22, 23, 24, 25, 26, 29, 31, 32, 33, 34, 53

PID Proportional Integral Derivative 22

List of Symbols

T_s model sampling time [s] 11, 18, 33, 43

Q_T turbine volumetric flow-rate, available at inlet [$\mathrm{m\,s^{-3}}$] 13, 15, 16, 17, 18, 33, 43, 44

E_k potential energy stored at the previous timestep OB [MW h] 13, 18, 43

$Q_{T,opt}$ optimal turbine volumetric flow-rate [$\mathrm{m\,s^{-3}}$] 13, 15, 41

$\eta_{T,max}$ maximal turbine efficiency [−] 15

η_P pump efficiency [−] 15, 16, 18, 34

η_T turbine efficiency [−] 16, 18, 20, 21, 25, 26, 27, 28, 30, 31, 32, 33, 34, 41, 47, 48

P_T operating power of the turbine [$\mathrm{J\,s^{-1}}$] 16, 18

ρ_f density of the fluid in the OB pipes [$\mathrm{kg\,m^{-3}}$] 16, 18, 43

g gravitational acceleration [$\mathrm{m\,s^{-2}}$] 16, 17, 18, 43

H_s static head that the pump is subject to in [m] 16, 17, 18, 21, 43

Q_P turbine volumetric flow-rate, available at inlet [$\mathrm{m\,s^{-3}}$] 16, 18

P_P operating power of the pump [$\mathrm{J\,s^{-1}}$] 16, 18

v_f the velocity of fluid in the turbine inlet [$\mathrm{m\,s^{-1}}$] 17, 43

K friction coefficient [−] 17, 43

A_i the area of the turbine inlet [$\mathrm{m^2}$] 17, 43

D depth of the OB, relative to sea level [m] 18

h height of the fluid in the OB reservoir [m] 18, 19

E_{out} energy generated by draining the OB [MW h] 18

$E_{out,p}$ potential energy which can be generated by draining the OB [MW h] 18

$E_{out,r}$ relative amount of energy generated by draining the OB, w.r.t E_{max} [−] 20, 21, 25, 28, 43, 44, 47, 48

E_{max} maximum energy capacity of an OB [MW h] 21, 41

T_d time to drain current volume [s] 33

V_c current volume of OB bladder [m] 33

Chapter One

Introduction

Growing concern over the threat of global climate change has led to an increased interest in research and development of renewable energy technologies (Pelc and Fujita, 2002). Recent research highlights that the size and number of off-shore wind turbines over the next decade is expected to rapidly increase due to the high wind energy potential; due to the fact that offshore wind turbines can capture higher wind speeds than onshore wind turbines (Qin, Saunders, and Loth, 2017). One drawback to renewable energy sources however is the intermittent and variable supply of energy (Kalogeri et al., 2017); this shortcoming is dealt with by the Ocean Grazer (OG) by integrating wind and wave energy and additionally on-site energy storage. Integrating wind and wave energy resources brings a less variable output with fewer hours of zero production, compared to production of an individual wind energy converter (Kalogeri et al., 2017). To store potential energy, the system pumps a fluid into flexible bladders that are deflated by the pressure of the ocean, deflation causes a turbine to recover this potential energy; this technology is referred to as the Ocean Battery (OB).

The OB is a standalone technology allowing for modular use. Hence, several OBs can be connected creating an OB network. An overview of the OG is depicted in Figure 1.1, note here that there are two OBs anchored to the ocean floor. The OB on the right stores potential energy, where the bladders are fully inflated, whilst the one on the left has deflated bladders and thus does not store energy.

Recently, a predictive model, fundamental in this research, deciding on the storage of energy has been developed in Python by a master student working on **revenue maximisation** for the OG (Niekolaas, 2020). Renewable energy from wind turbines is non-constant (Lira et al., 2016), energy storage allows for capturing favorable market price fluctuations in order to maximise revenues. This model will be investigated for its validity (Chapter 2) and complemented in this research such that it becomes more accurate, focus will be on investigating the efficiency losses involved with energy recovery using a Pump as Turbine (PAT),

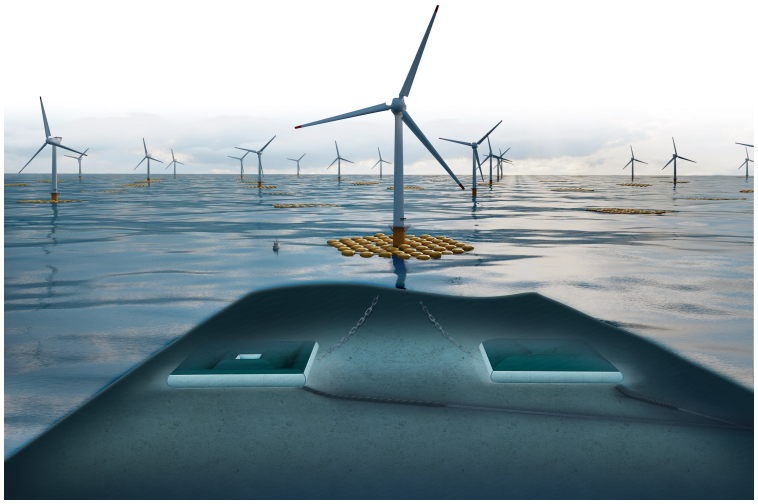

Figure 1.1 Overview of the Ocean Grazer and the connected Ocean Battery systems

a cost-effective energy recovery technology in pressurised water supply systems (Ramos and Borga, 1999; Delgado et al., 2019). This study will investigate the effect of including realistic efficiency behaviour on energy storing decisions of the Model Predictive Control (MPC) through curve fitting, relating stored energy to efficiency, provided turbine efficiency curves (Jain and Patel, 2014), and literature research on these PATs (Chapter 3). The current model predictive control strategy for controlling a network of OB systems is built on assumptions affecting efficiency; this entails that the model's validity and accuracy is to be investigated.

The remainder of this first chapter aims to provide a more specific outline of the problem. Essential to obtaining the particular researched problem is by identifying relevant influence of stakeholders and providing a clear description of the researched system. In order to solve the researched problem, a research goal, identifying research questions and the tools required to provide answers to those, the strategy and the planning of the research in a time-frame of twelve weeks. The remainder of this paper will be structured along the following lines: in the second chapter, the current model is validated using sensitivity analysis amongst others; in the third chapter, literature research of PAT is provided as well as explanation on how the current model is expanded; in the fourth chapter, results will be provided and discussed; in the fifth chapter, conclusions will be provided, as well as limitations and future recommendations.

1.1 Stakeholder analysis

Stakeholders, *i.e.* persons who may affect the project (Wieringa, 2014), are identified in order to understand the origin of the problem, in particular the problem owner. The problem owner is the Chief Technology Officer (CTO) of the Ocean Grazer company: Marijn van Rooij. He identified the following problem: *the current model is not validated and built on many assumptions.* The goal of the Ocean Grazer company is to deliver their product to the market. Mr. Van Rooij has high interest in the technological aspects of the OB and consequently in the validity and accuracy of the model. Revenue maximisation by the aforementioned control system of OBs provides competitive advantage to the OG in comparison with other renewable energy producing systems, as the control system allows for effective and efficient energy selling and storing decisions provided the behaviour within the energy market. However, it makes no sense to include a control system which is not validated; elaboration on limitations which cause the lack in accuracy is provided in Section 1.3. Mr. Van Rooij is the representative of the company (OG B.V.) and clarifies the company's perspective on the problem. Consequently, he has high power in the project as this project is devoted to improvement of the OB.

At the moment, two other stakeholders in this research are identified. Prof. dr. ir. Bayu Jayawardhana, the first supervisor of this research who is a part of the Ocean Grazer research group has influence in this research. The research in influenced in such a way that it is of sufficient quality in order to qualify for a bachelor's integration project; the tools and methods used throughout this research are influenced accordingly (elaboration on the methods are provided in Section 1.7). The third and last stakeholder is Wout Prins. He has two roles, one as project manager of the university and one as project manager for the OG company. Mr. Prins sees to it that the project is of sufficient scientific quality in order for it to be of potential added value to the company's technology as well as the university, such that particular findings of this research might be of future use in articles by others conducting research on the OG. Mr. Prins consequently has high power in the research as this research is devoted to improvement of the OB. The power of both Mr. van Rooij and Mr. Prins is hence exerted by providing direction to this research. The current stakeholder map is depicted in Figure 1.2. In the map, one connection between the stakeholders is identified, depicted with enumerated arrows which have been explained below.

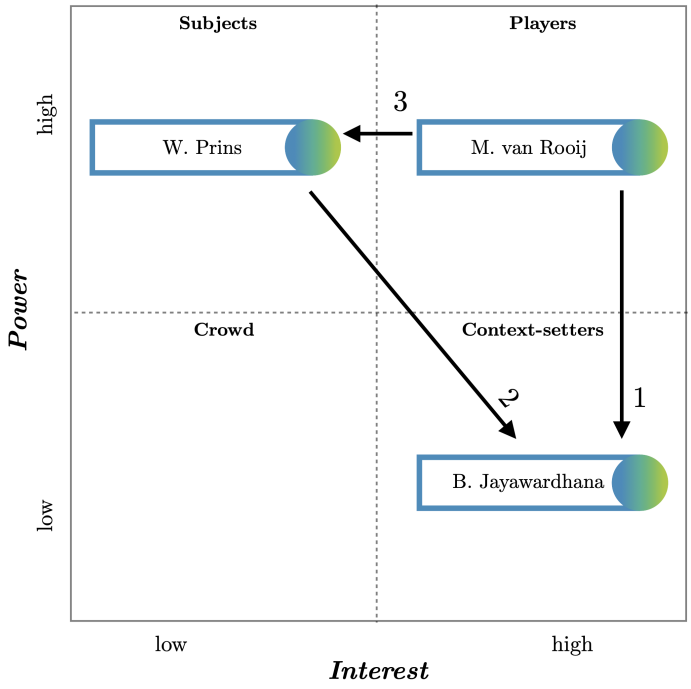

Figure 1.2 Stakeholder map

1. Mr. van Rooij has power in the outcome of this research as he is the problem owner; Mr. Jayawardhana is influenced by potential direction provided to this research by Mr. Van Rooij.

2. Mr. Jayawardhana is influenced by potential direction provided to this research by Mr. Prins.

3. M. van Rooij is CTO in the company; given his high interest and power in the technological aspect of the research, this affects advice provided by W. Prins.

Currently, no other stakeholders are identified. Deployment of the OG in the market would potentially bring "new" other stakeholders.

1.2 System description

The model deciding on energy storage has been developed in order to allow for selling energy at higher rates than the current. In Figure 1.3, a graphical overview of the high level system is provided *i.e.* all intermediate stages of energy, from the generation of renewable energy to end-user electricity supply; these are depicted in blue. Additionally, the control decisions

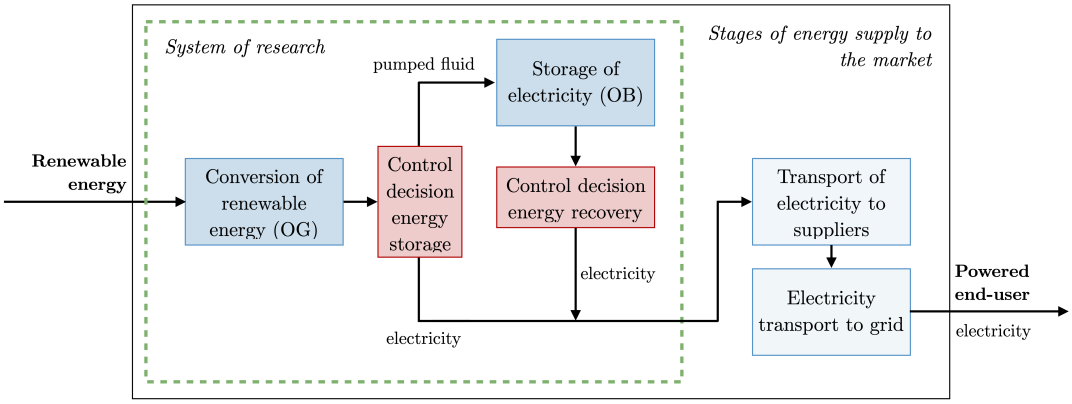

Figure 1.3 Graphical overview of the high level system

have been depicted in the figure in red. The control system decides on what happens to the converted renewable energy; the electricity could either be used to inflate the bladders and accordingly store potential energy, or directly transported to energy suppliers.

The OB consists of several sub-functions. In Figure 1.4, a more detailed overview of the system is provided including the aforementioned sub-functions such as the mechanical actions, control decisions and a stored energy state. The three main mechanical sub-functions (depicted in dark blue) of the OB display how potential energy is stored and recovered. The potential energy stored is visualised in green, as this is no real action, nevertheless it is important for the reader of this thesis to grasp. The control system (depicted in red) decides on the energy storage. The control model receives information inputs (dashed line) such as the number of wind turbines, the number of OBs, energy market prices and the current energy stored in the network.

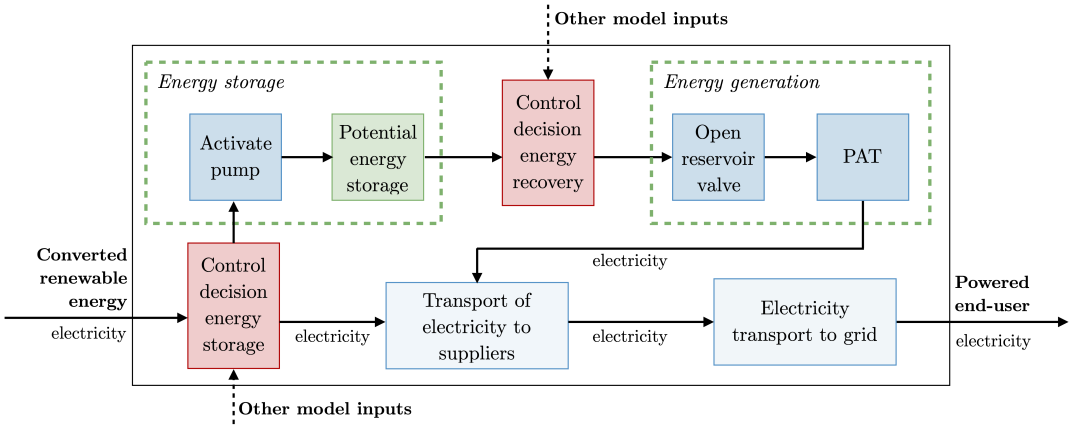

Figure 1.4 Low level graphical overview of the system

Now that it is clear how the control model interacts with the system, an image of what the system will look like is provided in Figure 1.5. This is an illustration of the side-view of the machine room between the inner (left) and outer (right) reservoir tubes as provided in Figure 1.1. The reservoir tubes, which have a little amount of water in them in this figure are connected, with pipes (purple), to the spiral-shaped pump (in turquoise/light blue). The pump has a tube attached to it, which extends to the empty space above the machine room, this is where the aforementioned bladders are.

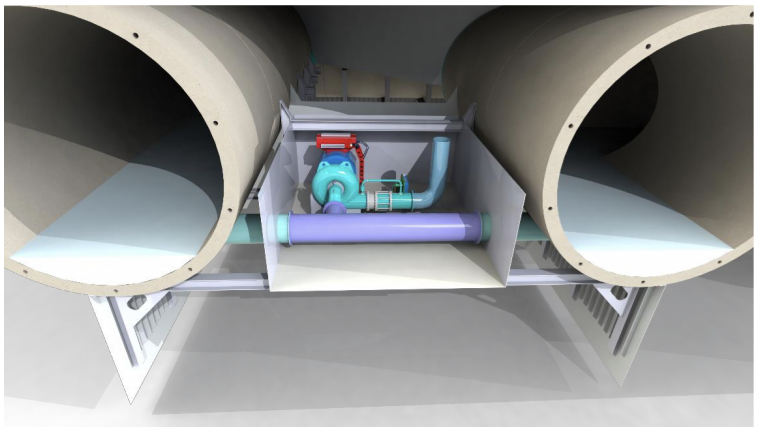

Figure 1.5 Side view of the machine room of the Ocean Battery

The control decisions, on storing and transportation to the grid, are logically based on the outcome of the model. However, those decisions are not founded upon a validated model. In Subsection 1.2.1, the limitation which is argued to have the greatest influence on the models accuracy will be discussed and subsequently included in the system of this research. The first cause of the main limitation has been identified by the problem owner, whereas the second limitation stems from reasoning on the existing model, as efficiency is assumed to be high. The problem owner sees this fifth limitation to be of significant impact on the efficiency of energy storage, supporting that it is to be researched.

1.2.1 Limitations current system

The most important limitation is that rather high efficiency of energy recovery in the OBs is assumed in order to generate convincing figures compared to situations without the OBs. The identified problem is that those energy losses are not taken into account in the current situation. Part of this efficiency loss is traced back to the underwater dynamics and pressure differences causing the efficiency to varying over time. This will be covered in Chapter 3.

It is also argued that the PAT start-up procedure causes significant efficiency loss. The starting procedure influences the storing capacity of the system. Time is required to reverse the pump in order to make it function as a turbine and to reach its full potential again, which is the start-up time (Nicolle, Giroux, and Morissette, 2014). The pump functioning as a pump has to deal with start-up (its transient response) due to fluid inertia, and so does the PAT. Power is lost with these start/stop cycles, *i.e.* when electricity is used to inflate the underwater bladder and again reversed to generate energy, since it will take some time for the actual flow-rate of the fluid to reach its Best Efficiency Point (BEP). The fact that each start/stop cycle will cause a loss of energy which was to be stored, it is very inefficient to let the control model decide for small time instances to recover energy by deflating the bladders of the OB. The flow-rate and velocity of the runner (blades within turbine) provides for a fluid inlet profile in the bladders causing limited swirl (Nicolle, Giroux, and Morissette, 2014). This limited swirl is inefficient as the maximum power of the pump is present but not converted into a maximum flow-rate. This process initiates a loss of kinetic energy.

1.3 Scope

This research is focused on evaluation and improving the existing control model. In consultation with the problem owner, and by into account limitations mentioned in the previous section, this research will focus on efficiency losses caused by using PATs. Sub-questions will be conform to the investigation of these efficiency losses and explanation on the assessment of the losses will be provided in Subsection 1.6.1 and Section 1.7 respectively.

1.4 Problem statement

An elaborate problem background is provided in the introduction and the system description, Chapter 1 and Section 1.2 respectively. The problem statement is provided below this paragraph. In Section 1.3, it is provided why this particular problem is selected from the problem context. Currently, convincing but inaccurate results are generated. Including the yet to be investigated limitation is argued to add significant accuracy to the control model.

The existing predictive control model incorporates the assumption of high efficiency in the energy recovery state of the OB, i.e. the use of a PAT; this entails that the model's validity and accuracy is not guaranteed.

1.5 Goal statement

This is practice-oriented research, as the research is focused on understanding the limitations of the current control model and to improve it, likewise providing knowledge and information that can contribute to a successful intervention (Verschuren, Doorewaard, and Mellion, 2010), the intervention in this case is related to the improving the model. The focus of this research will be on the PAT and its influence on energy storing and recovery efficiency. The goal of this research naturally arises from analysis of the current model, it is stated hereafter.

To improve the accuracy and validity of the existing model, by implementing the operation characteristics of using PATs in the current model, as the exclusion of this limitation currently causes significant efficiency bias.

1.6 Research questions

This research is built upon one central research question, which is to be answered by providing sufficient information beforehand, in compliance with the project goal.

What is the effect of including efficiency loss due to the use of PAT on the revenue optimisation process?

1.6.1 Sub-questions

In order to provide an answer to the central research question, sub-questions are formulated. The answers to the sub questions contribute towards solving the central research question.

1. Does the current model need more validation?
2. How does the existing model predictive control strategy perform in optimising revenue?
3. What is the influence of the PAT on energy storing efficiency?
4. How do different PATs behave in terms of startup times and power loss?
5. How do PATs perform compared to standalone pumps and turbines?
6. How is PAT efficiency influenced when the OB network is scaled up, *i.e.* generalisation for larger a scale networks?

1.7 Tools and methods/Research materials

This section provides proposed tools and methods for obtaining the required knowledge for answering each of the aforementioned sub-questions.

1. The first sub-question is answered by studying the validations section of the masters research by Kirsten Niekolaas, who developed the mathematical control model (Niekolaas, 2020). It is also important to discuss validity with stakeholders.

2. The second sub-question is answered by studying the outputs of the existing code. A sensitivity analysis is to be performed such that the amount of variation that the system has in response to specific range(s) of input can be observed (Simske, 2019). Additionally, it is needed to understand how revenue is maximised, which is done by identifying which parameters are maximised and minimised leading to this maximised revenue.

3. The third sub-question is answered by studying literature on the PATs and possibly implementing this in the model such that the actual effect of draining efficiency can be understood. Relevant literature relating to PAT efficiency was conducted by A. Carravetta, 2018; Breeze, 2018 and Jain and Patel, 2014 among others. This sub-question relates directly to the central question. Having insights in the extent to which storage is affected allows for implementation in the model and thus the effect on the revenue optimisation process.

4. The fourth sub-question is answered by studying the available PAT solutions listed in literature. Extensive research has been conducted among numerous alternatives by A. Carravetta, 2018.

5. The fifth sub-question is answered by studying literature on standalone turbines and comparing those to PATs. Those turbines will be compared on efficiency, volumetric flow rates and the head of the structure.

6. The sixth sub-question is answered by an equal approach as the one proposed in answering the second sub-question, *i.e.* by sensitivity analysis. This analysis primarily focuses on increasing the number of batteries per network/the number of wind turbines per battery, whilst a simple set-up would suffice for investigating the second sub-question. This allows to clearly distinguish the influence of the connected network isntead of the dynamics of single OBs.

Chapter Two

The existing model

The control model in Python, which is developed by Kirsten Niekolaas is used throughout this research. Several sub-questions are focused on the performance of the current model, in particular the first two sub-questions. The performance and accuracy of the existing model is assessed as follows: the model is analysed in Section 2.1 and subsequently, in Section 2.2 the need of extra validation of the current model is discussed.

2.1 Analysis

Irrefutable evidence on the use of MPC in this setting has been provided in previous research. In accordance with previous research on the OG, a definition for optimised revenue is derived. The OB provides the OG with the advantage to produce energy almost instantly on demand, enabling the OG to sell energy when there are for example high price peaks on the electricity market (Dijkstra, 2016, p. 5). The use of MPC allows for the OG to generate higher revenues, when energy prices are available one day in advance.

2.1.1 Energy markets and prediction horizon

Background information on the two energy markets, day-ahead and the Automatic Frequency Restoration Reserves (FRR) market, which have been investigated proves useful as it explains the price behaviour of the data over time and allows for picking a credible prediction horizon, that is the period of time for which the price is available to the model in advance.

The FRR market finds its roots in the following problem: an ever increasing availability of renewable be energy which is highly inconstant as mentioned in Chapter 1. This inconstant supply of energy alters the mains, or utility frequency. Whenever energy demand exceeds the supply, the frequency becomes too low and along these lines will the frequency be high when the supply exceeds demand. If this mains frequency is too unbalanced, a blackout in

the grid might be the consequence. The consumer side of the energy market has also proven to be highly varying, this creates significant imbalance in the Dutch power grid in particular (NextKraftwerke, 2020). The sub-sector of this FRR market on is automatically restoring the mains frequency (aFRR). A Balance Service Provider (BSP) may bid on energy, these prices are variable and may also be negative, this is where energy storage of the OG will prove highly useful. The bids have to be made available one day ahead in the afternoon, namely before 2.45 p.m., in the aFRR market according to article 10.38 paragraph 1 "Netcode Elektriciteit" from the Dutch law (Overheid, 2020). This allows for quite a large time window to adjust decisions and thus rather large prediction horizon. The downside is the uncertain demand, one scenario might be that the very little energy is requested in very sunny and windy conditions, causing prices to become negative. In this worst case, it might cause the storage to become completely filled at one point which leaves selling energy at negative prices. This however is very unlikely, in for example Finland, the grid suppliers state that aFRR is mostly used for demand in certain morning and evening hours, which are informed in advance (Vänskä, 2020). This market thus might be interesting to investigate in future research, because higher demand in the morning and evening hours might in its turn drive the energy price.

Now, due to the energy prices being available on the preceding day, a prediction horizon of over 9 hours. With a T_s of 1800 s, *i.e.* one half hour, the prediction horizon can be at least 18 in the aFRR market. This entails that the model will have the energy prices of the upcoming 18 instances available at all times.

2.2 Validation

Currently, the validity of the model has been tested by using a software package which conducts a sensitivity analysis. This however does not have to entail that the model is valid and accurate and hence, the reason why manual sensitivity analysis will be conducted on the model. As mentioned in the tools required for the third sub-question (1.7), a stripped down version of the direct model will be used for analysis on the amount of stored energy caused by price changes, input energy variations, differing set-ups w.r.t. the number of OBs. This is due to the following hypothesis, which is yet to be validated, that losses of transferring energy between OBs will cause the system to incur high energy losses when deciding to store energy in consecutive batteries, and again deal with losses when this energy is transferred back to the grid passing through each battery in-between. It is hypothesised that the amount of revenue will decrease drastically as the number of OBs and clusters is increased due to

energy losses which occur in distributing energy along different batteries. Therefore, one of the analysis will consist out of a sensitivity analysis on the losses in the indirect model. Note that, for all simulations the sampling time of 1500 seconds will be used. From Niekolaas, 2020, it has become clear that sampling time varying from 0.01 to 3600 had no impact on the round-trip efficiency simulations.

In this subsection, a manual sensitivity analysis will be conducted on the indirect model and especially the extent to which these affect the model storing behaviour and revenues. It is hypothesised that the indirect will be less likely distribute the energy among other batteries in the network, as losses are incurred both when storing and recovering energy. The variables which will be tested for parameter variability are the number of storages and the number of storages in one cluster. A cluster consists of a number of OBs which are all kept at the same storage level. It is a lumped model of N OBs and thus N times the capacity of one OB. The number of storage units in a cluster determines the total amount of energy that can be stored. In previous research, the size of the cluster is researched to determine the suitable number of OBs per wind turbine. Accordingly, the number of storage units per wind turbine has been set to be 3 to match the energy production of wind turbines. Varying the number of clusters yields increased storage, as the energy is spread equally among all the storages in that cluster and the storage capacity is increased significantly. However, increasing the number of storages will cause the individual storage levels to go to zero rather quickly. Namely, increasing the number of OBs with 1, so 5 instead of 4, will yield zero storage among the system over the entire simulation time, that is, provided the produced wind energy data.

Decreasing the pump efficiency to 90%, instead of the initially used 95%, will decrease the storage by 45%, or from 28.1 to 15.5 MW h in an absolute sense. When investigating even lower pump efficiencies, it becomes clear that no energy will be stored. However, this could be caused either by the low efficiency, *i.e.* that energy is indeed stored but much is lost, or by the fact that energy storage is deemed unprofitable by the MPC. It turns out that the second statement is true, very little energy is stored (in the range of 10^{-8}) at a pump efficiency of 85%, almost all energy is directly sold after receiving.

Altering the turbine efficiency, has an even greater effect on energy storing decisions: decreasing the turbine efficiency to 90% will yield a decrease in storage of around 62%, from 28.1 to 10.8 MW h. The threshold for significant energy storage, *i.e.* in the range of 1 to 7.3 MW h has been reached with a turbine efficiency of around 86%. Turbine efficiency below that level will yield no energy storage.

Now, due to the fact that turbine efficiency will be investigated and accordingly lowered, it will be a challenge to generate convincing results with these lower efficiencies. This might entail that the system will have to be "promoted" to store energy in order to understand the effect of efficiency, which is subject to change at different levels of stored energy. Chapter 3 elaborates on the investigation of efficiency in the pumping system. So resulting from the first sub-question, as this research is focused on investigating the effect of including efficiency loss due to PAT, it has been useful to investigate the range of efficiency for which the model generated results.

It is hypothesised that energy storage will peak when the price would suddenly drop, provided that the price would suddenly increase directly afterwards. This indeed holds true, pledging in favour of the validity and accuracy of the model. However, when this happens in combination with the turbine efficiency being lower than its previously mentioned threshold, no energy will be stored. Revenues are to be maximised by storage even with lower efficiencies, however then the storage must be promoted by gaps in the energy price.

2.2.1 Use of Matlab turbine model

In order to understand whether if previous research (Van Kessel, 2020) meets the mathematics behind the MPC, an expression relating flow-rate and stored energy will be derived analytically in Equation 3.7 to B.2 in Appendix B. This will be done using the draining dynamics obtained from literature in Section 3.1. Subsequently, the Matlab turbine model by Thimo van Kessel, hereafter referred to as the Matlab model, will be executed in order to obtain data relating flow-rate and stored energy. Then the a curve with the expected behaviour will be fit to this data in order to validate simulation results. It is presumed that the average flow-rate increases proportional to a third degree root of stored energy during drainage phase, $Q_T \propto \sqrt[3]{E_k}$.

Efficiency values are highest at their BEP (Van Kessel, 2020). This might seem trivial, it is however in line with efficiency curves found in (reviewed) literature (Bansal, 2017; Jain and Patel, 2014), as the current flow-rate is compared to the system's optimal flow-rate ($Q_{T,opt}$ for turbines), *i.e.* at BEP. This leads to the conclusion that the flow-rate behaviour is based on valid and solid scientific knowledge. The basis of the fluid motion is Bernoulli's principle which is focused on the impact of pressure difference and velocity behaviour which is the pillar for the bladders to in- and deflate at depths of the ocean, *i.e.* with higher pressure. Friction in both the piping system and the flow of the fluid have been taken into account, the foremost limitation of his research is that it has not been validated in practice. Though,

the flow-rate behaviour is a credible and logical representation of the draining and pumping phases of the OB which is why this research will be used for determining efficiency behaviour and relative energy storage levels.

Now, one might argue that the expression for turbine efficiency will be inaccurate due to the fact that flow-rate and head are time-varying variables causing the efficiency to vary over time during the draining phase. This might be pointed to as a limitation of the research, which will be covered in Section 5.2. This limitation is intertwined with disregarding Computational Fluid Dynamics (CFD), which is covered in that same chapter.

Chapter Three

Pumps as turbines

This study provides new insights into the behaviour of pumps working as turbines. As a result, the third to sixth sub-questions will be covered in this chapter.

3.1 PAT efficiency

Using a PAT is as a cost-effective solution for energy recovery in pressurised water supply systems (Delgado et al., 2019). Using PAT instead of standalone turbines comes with disadvantages, one of which is the efficiency profile. Many researchers have developed the relations for PAT efficiency w.r.t. relative discharge based on theoretical, experimental and numerical investigations (Jain and Patel, 2014, p. 658); these are depicted in Figure 3.1. Conventional turbines have wide operating range between 20% and 90% of their optimal discharge, *i.e.* $Q_T/Q_{T,opt}$, whereas the PAT (in red) works with higher efficiency in the discharge range of only around 80% to 100% (Steller et al., 2008). Hence, the applications of PAT are recommended at close to full load operation for maximum attainable efficiency (Jain and Patel, 2014; Derakhshan and Nourbakhsh, 2008). It is proven that the maximum turbine mode efficiency is equal to, or somewhat less than that in pump mode, *i.e.* $\eta_{T,max} \approx \eta_P$ (Williams et al., 2003; Derakhshan and Nourbakhsh, 2008). However, when the pump does not operate optimal, *i.e.* not close to full load, the PAT efficiency suffers great losses. The remainder of this section is dedicated to understanding the mathematics behind PAT efficiency. The efficiency term expression for both turbines and pumps includes mechanical losses and volumetric efficiency (Venturini et al., 2018). Equation 3.1a reads as: available power divided by the supplied power as provided in for turbines, or PATs. Whilst the opposite holds for pumps, Equation 3.1b is supplied power over available power. The available power is the actual power which is translated from the pump or turbine operation.

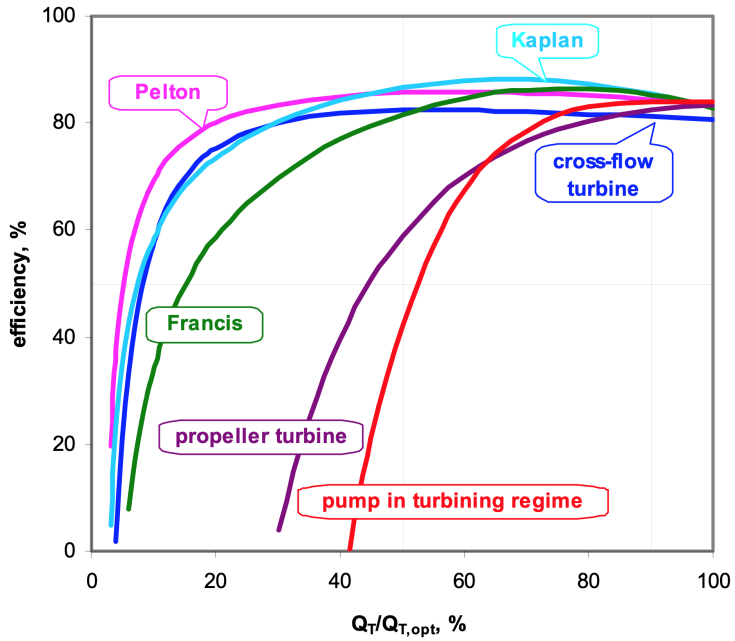

Figure 3.1 Comparison of the efficiency curves of different machines with respect to dimensionless flow rates (Steller et al., 2008)

$$\eta_T = \frac{P_T}{(\rho_f \cdot g \cdot H_s \cdot Q_T)} \tag{3.1a}$$

$$\eta_P = \frac{(\rho_f \cdot g \cdot H_s \cdot Q_P)}{P_P} \tag{3.1b}$$

3.1.1 Current implementation efficiency

Important to note is that the existing MPC incorporates a constant pump and turbine efficiency has been provided. The proposed parameters of efficiency are 85% and 90% for pump and turbine operations respectively. However in the model, efficiency of 95% is used for both pump and turbine operations in order to generate desired results, *i.e.* significant energy storage and thus increased revenues.

Van Kessel uses efficiency constants of both the turbine and pump and investigates round-trip efficiency, which is variable provided different flow-rates. The constants used represent the translation from kinetic to electrical, or vice versa, energy. A motor is used to power the pump, and thus rotate the runner blades, this is where the constant pumping efficiency term comes from. For turbine operation, that same motor is used as a generator, where the

constant turbine efficiency term is involved. Thus mechanical losses and volumetric efficiency have not covered with these constants, whilst Figure 3.1 and both the efficiency equations combine all the power losses present in the system, thus these efficiency values will not be multiplied with the motor efficiency. This is because of the fact that power input compared to measurable output already encompasses this efficiency. However, as mentioned before Van Kessel investigated round-trip efficiency of the OB and found efficiency curves, accounting mainly for both mechanical and volumetric head losses.

3.1.2 Pump and PAT dynamics

In order to understand how the efficiency behaviour emerges and how can be linked to model outputs, elaboration will be provided on the draining and pumping dynamics of the system in Section 3.2. The equation for the velocity of the drained fluid is derived using Bernoulli's principle, relating fluid velocity and pressure. This derived equation is known as the Torricelli law expressing the velocity of fluid flowing out of an opening related to the height of the fluid column above the opening, or the static head H_s (Dijkstra, 2016; Van Kessel, 2020). Static head, is the vertical difference between the surface of the water level in the reservoir and the sea water level (3.6). The expression for fluid velocity in the turbine reads

$$v_f = \sqrt{\frac{2 \cdot g \cdot H_s}{1 + K}}, \tag{3.2}$$

this velocity is directly proportional to the draining flow-rate, as it is multiplied with a constant (the inlet area of the turbine) (3.3). For completeness, a friction term has been introduced (3.2), representing surface friction the pipes. Note that this friction involved in this particular situation is treated as a constant over time and thus will not dynamically affect the efficiency behaviour, whilst the head does.

$$Q_T = A_i \cdot v_f \tag{3.3}$$

Consequently, the behaviour of the flow-rate is directly proportional to the square root of the change in head given Equation 3.6, *i.e.*

$$Q_T \propto \sqrt{H_s}. \tag{3.4}$$

Static head increases during the pumping stage since the water level in the reservoir decreases, while depth of the OB w.r.t. seawater level, remains the same provided Equation 3.6. Due to the increased head, the pump will have to deliver more power to pump a cubic meter of water to the bladder which can be seen in Equation 3.5; this is a rewritten version of the efficiency equation (3.1b). The power input of the pump remains constant, this will result

in a decrease of the pumping flow-rate. Required inputs to calculate the pumping power are pumping efficiency, density of the pumped fluid, pumping flow-rate and the static head respectively.

The opposite holds during the PAT phase, the fluid height in the reservoirs increases as the bladder's volume is drained into the reservoir, causing the static head to decrease. Consequently, the turbine flow-rate decreases during the PAT phase due to the aforementioned proportionality (3.4).

$$Q_P = \frac{\eta_P \cdot P_P}{\rho_f \cdot g \cdot H_s} \tag{3.5}$$

where

$$H_s = D - h_r \tag{3.6}$$

The previously listed equations have been applied in the model by Niekolaas and are used to determine the amount of energy which is stored and recovered. When the model decides to sell its stored energy, the recovered energy is calculated using Equation 3.7a and Equation 3.7b.

$$E_{out} = \eta_T \cdot E_{out,p} \tag{3.7a}$$

where

$$E_{out,p} = \begin{cases} \frac{T_s}{3600} \cdot P_T, & E_k > \frac{T_s}{3600} \cdot P_T \\ E_k, & \text{else} \end{cases} \tag{3.7b}$$

Now, combining these equations yields an expression relating stored energy and change in head during the draining phase as well as the average flow-rate. the average flow-rate will increase proportional to a third degree root of stored energy during drainage phase, *i.e.* $Q_T \propto \sqrt[3]{E_k}$. Analytic derivation of this proportionality has been provided in Appendix B. These mathematics behind draining serve as a check whether if these obtained dynamics match the modeling of flow-rate behaviour from Van Kessel. It is checked by curve fitting a cubic root to the obtained data. Explanation on that curve fitting procedure has been provided in Section B.1.

3.2 Implementation of varying efficiency

Decision making of the model predictive control system is hypothesised to be affected by the implementation of PAT in the model. When including for example the efficiency curve, the model might opt for higher utilisation of storage use instead of often discharging due

to attractive market prices: as the efficiency of using PAT is relatively low at low discharge rates. This section provides insight in the context third sub-question and ought to answer this question accordingly.

In order to provide generalised implementation of PATs in the model, the model is to receive as an input the type of turbine, *i.e.* their discharge efficiency curve. This makes the model easy in use and allows the user to easily distinguish between several PAT options. In Section 3.1, it is proven that PATs are recommended to operate close to full load discharges in order to provide sufficient efficiency. This entails that the number of discharges will be limited in a sense that discharges below the operating range for PATs yield great loss of energy. Hence, the decision making of the model predictive control system is influenced. In the subsequent paragraph, elaboration on the draining conditions will be provided and subsequently the influence of varying efficiency during drainage from different values for head.

Currently, the model output at every iteration is an array with the stored energy in every OB in the connected system. In the following sections, a relationship between stored energy and average efficiency of draining will be obtained. Hence, it would allow the model to estimate the efficiency when the bladders would be drained at that particular point in time. As stated before, with PATs recommended to operate close to full load discharge. However, this entails that first the discharge range must be determined at varying values of head and thereafter for levels of stored energy. An estimation of the draining conditions w.r.t. flow-rate and thus efficiency can be made using the Matlab model. This model calculates during pumping and draining the behaviour of flow-rate, power and efficiency, among others, for an OB at 40 m depth. Simulations for varying values of head were conducted such that the behaviour of the aforementioned parameters can be determined. The code has been complemented such that the parameters which are of particular interest for this research are easily obtained. Explanation on which is covered in Appendix A. The methodology of obtaining the desired data using the complemented Matlab model is listed in Subsection 3.2.1, all required data on the average turbine efficiency provided a particular energy storage level is obtained through execution of this methodology. A scatter plot of the data has been provided in Figure 3.2. The operating head in the researched and proposed setup of the OG ranges from 31 to 40 m due to the reservoir height ranging from 0 to 9 m as stated in Section 3.4. This allows for explaining the behaviour of the data for energy storage less than approximately 6.3%: this is the lower storage limit beyond which storage is not possible since the h approaches 0 m. Therefore, draining in this region yields 0% efficiency, as it is impossible. In accordance with the advisor and stakeholder of this research, a non-linear curve will be fit to the obtained efficiency data using Python. This is essential to allow implementation in the MPC. The

entire curve fitting procedure is explained and the script has been provided in Section C.1 of Appendix C. Subsection 3.2.2 lists the required methodology for obtaining the non-linear curve.

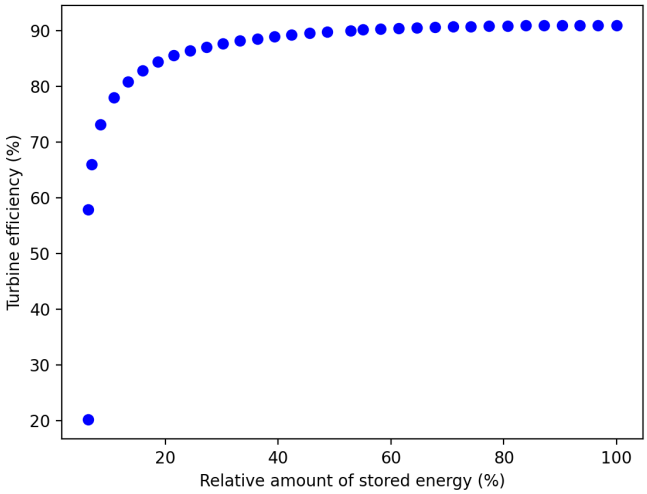

Figure 3.2 Efficiency corresponding to relative amount of stored energy

The curve fitting has been done through the use of Python and elaboration on that procedure has been provided in Section C.1. The obtained function reads as

$$\eta_T = \begin{cases} 0 & 0 \leq E_{out,r} \leq 0.063 \\ -0.43 \cdot |E_{out,r} - 0.050|^{-0.52} + 0.95 & \text{else,} \end{cases} \tag{3.8}$$

due to the limited domain of the natural logarithm, as its input can never be zero. It has been depicted in Figure 3.3. Provided this curve fit expression, it becomes clear that for a rather large range of stored energy will the efficiency of drainage be sufficient for energy recovery. This is mostly caused by the depth of the OB resulting in a large enough pressure difference to drain. Appendix C provides explanation on all used methods and generated results which are provided in this section. At each iteration, the efficiency will have to be determined for every OB in the distributed energy network separately. Therefore, this function must not be very computationally expensive, as it presumably would then take much time to determine the efficiency for all batteries.

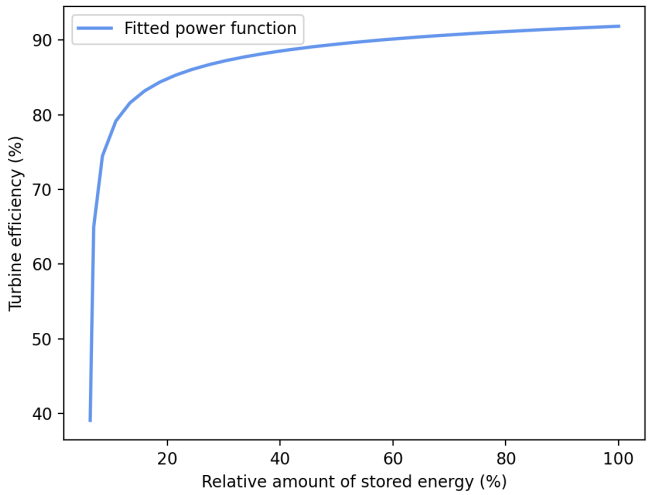

Figure 3.3 Graph of function relating stored energy and draining efficiency

3.2.1 Methodology of obtaining data using existing Matlab model

1. Initialise head, H_s, and determine E_{max}.
2. Find relative amount of drained energy, $E_{out,r}$ and average η_T and store this collected data in two arrays, x and y respectively.

3.2.2 Methodology of curve fitting in Python

1. Plot x and y from Subsection 3.2.1 on the corresponding axes 3.2.
2. Guess function (several functions are tested).
3. Guess parameters.
4. Use Python curve fit package to determine optimal parameters for least squares optimisation.
5. Plot fitted curve 3.3.

Execution of this methodology yields a non-linear curve linking turbine efficiency to a particular amount of stored energy. This is to be implemented in the existing Python MPC (Niekolaas, 2020), such that efficiency is to be estimated at particular storage levels.

3.3 PAT start-up procedure

Every time the OB recovers its stored potential energy, the turbine has to respond to the incoming flow and this reverse motion will trigger generator to recover electric energy. With responding to the incoming flow, it is meant that the rotating frequency of the turbine blades start turning in such a way that generated power is optimal. This is where the fourth sub-questions originates from. Previous research on turbine-governor systems has shown that there is a direct relation (a cubic polynomial to be precise) between mechanical power and guide vane opening (Zhao et al., 2018). The actual starting procedure follows S-shaped behaviour (Casartelli et al., 2019).

Many research has been done on power response of hydro-power systems, which is required in order for energy suppliers to qualify for delivering energy to the FRR markets (W. Yang et al., 2016; Guo and J. Yang, 2018). The goal for these energy suppliers is to deliver energy as soon as possible, after it being requested, to balance the mains frequency. In Europe, regulations for these power reserves are the following: if the rated head of the unit is larger than 50 m, the power delay time should be less than 4 s (W. Yang et al., 2016). Another regulation The most crucial requirements are: the power adjustment quantity should reach 90% of the static characteristic value within 15 s (W. Yang et al., 2016). Guide vane opening is specific for Francis turbines, controlling the angle of these vanes is used to control the incoming flow in the turbine. In this manner can the specific speed of the turbine indirectly be controlled during the entire draining operation. In addition, specific research has been conducted on the transient start-up for PATs, through the use of CFD (Casartelli et al., 2019). In this research, the guide vane angle was adjusted to minimise the power response time using Proportional Integral Derivative (PID) control, causing optimal flow behaviour and avoiding drawbacks such as water hammer and cavitation, these have been excluded from the research, as well as (fluid or turbine) inertia and will therefore be discussed in Section 5.2. Now, due to the aforementioned regulations, a start-up time of 2 s will be assumed in which no power is produced, as the 4 s response is an S-shaped curve (the area under which can be approached as a triangle), where power output is thus not optimal but not zero either. Therefore, a draining time penalty of 2 s, where there is zero power output is assumed, is used.

3.4 PAT versus standalone turbines

Research has been conducted on the relations of pump selection with respect to turbine efficiency (A. Carravetta, 2018, p. 60). Manufacturers tend not to provide efficiency curves for

PAT usage (Jain and Patel, 2014). However, much research has been conducted on ranges where specific applied turbines perform reasonably well. Results of this research has been depicted in Figure 3.4. In the researched OG setting, head ranges from 31 to 40 m and the bladders are drained with flow-rates up to 5 $m^3 s^{-1}$. Taken into account those parameters, turbines which operate closest to PATs can be identified from Figure 3.4. Francis and cross-flow turbines seem to fall within the OB operating ranges of the aforementioned parameters.

In comparison with standalone hydraulic turbines, PAT does not have guide vanes, causing the blades' speed to vary according to the varying power output. This may lead to instabilities in PAT at part load and results in poor part load efficiency, which is one of the major issues impeding the PAT technology (Jain and Patel, 2014). Also, this limitation does not allow for controlling the incoming flow in the turbine as much as would be possible with Francis turbines. Now, only the flow can be regulated with the relative valve opening. The possibility of controlling the incoming flow has been discussed in Section 3.3.

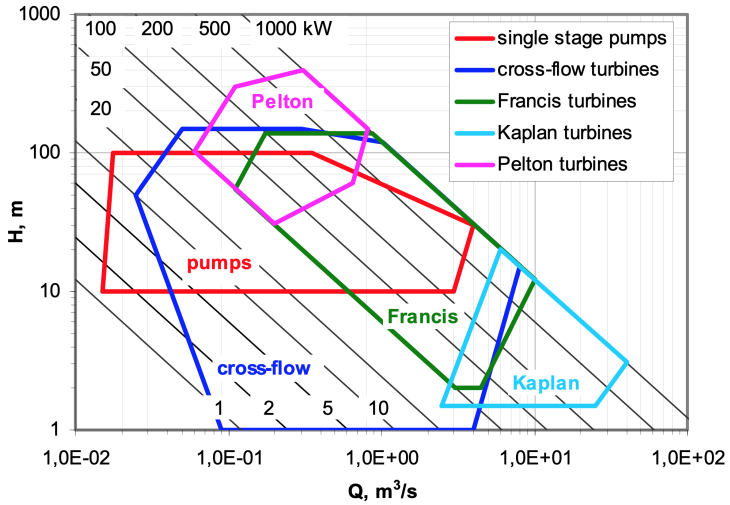

Figure 3.4 Typical application range of single-stage pumps in turbine mode of operation from Steller et al., 2008

3.4.1 Francis turbine versus PAT

Investigation on the performance of PAT versus Francis turbines, *i.e.* a turbine for which the operating range is suitable, is done using exactly the same methodology of Subsection 3.2.1 and 3.2.2. Hence, will the fifth sub-question be answered. The only difference for investigation of Francis turbine efficiency that the efficiency array in the function `N_T` has been altered to match the efficiency curve of Francis turbines instead of PATs, as provided in Figure 3.1.

This function, `N_T`, is used in `roundtrip.m`, *i.e.* in the Matlab model, to obtain the efficiency provided the flow-rate as its input and can be accessed by typing `edit N_T`, the `D`-array represents the efficiency curve in the model. Curve fitting, as provided in Section C.1 has been conducted on the obtained data. This results in the curve-fit depicted in Figure 3.5. In this figure, the curve fit of PAT has been provided alongside the one of the Francis turbine. The main conclusion which can be drawn from Figure 3.5 is that the Francis turbine manages to grasp significant higher efficiency at lower energy storage levels. However, at higher levels, the PAT manages to grasp equally high efficiency. The main advantage from using a PAT is that it can be used for pumping as well. This entails that it one fewer machine will become vulnerable for maintenance and failure, which is undesirable as the OB is located at 40 m depth. Also additional piping will be required for using standalone turbines, as flows of pump systems will logically be in opposite directions, increasing the complexity of the underwater structure. No more elaboration will be provided on using standalone turbines in this research, however it might be of interest for future work.

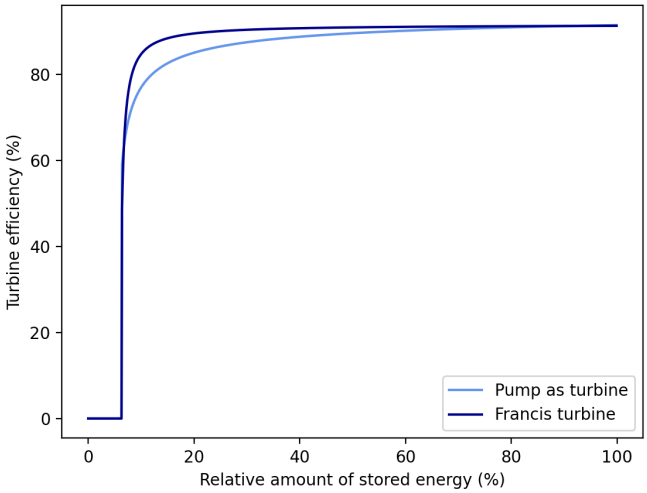

Figure 3.5 Turbine efficiency of PAT versus standalone (Francis) turbine

Chapter Four

Results and discussion

The first investigation on the influence of draining efficiency, *i.e.* the integration of sub-questions 3 to 5 will be discussed in this chapter. The existing MPC is designed with primary focus on researching the network of interconnected OBs and generators. In order to clearly distinguish the effect of efficiency on storing behaviour, instead of the effect on storage in a network of connected OBs, the model will be down-scaled to 1 OB, 1 generator and 1 wind turbine; as explained in the methods for the third sub-question in Section 1.7). Elimination of the network of batteries will allow for answering the third sub-question without incurring losses in the system due to interconnections, or the lack of connections to the grid proscribing the model from selling energy from a particular battery: as a single battery is free to store and drain, and consequently sell, energy at any given time.

4.1 The improved model

Literature research on draining efficiency behaviour, provided a specific amount of stored energy, is provided in Section 3.2. The existing MPC has been down-scaled and complemented with this varying efficiency. As expected from Section 2.2, when implementing the more accurate, *i.e.* lower, efficiency curve, storage decreased. Promotion of storage gives insight into the altered decision-making of MPC, and it is proven that the implementation was successful. Every iteration, $E_{out,r}$ is determined based on previous iterations and correspondingly, so is the η_T. Revenues turn out higher and the MPC now decides to **drain less often** but quicker, as this is penalised through efficiency curves.

Currently, the model has been generalised in such a way that the user can decide whether a PAT or standalone Francis turbine will be used for the simulation. This choice changes the efficiency function from Subsection 3.4.1.

4.1.1 PAT versus standalone turbine

In Section 3.4, a standalone, Francis in particular, turbine was investigated for its efficiency compared to PATs. Additionally, a curve was fit to the obtained data in Python. When the model runs using the efficiency function corresponding to the Francis turbine, revenues turn out little higher. Which was expected due to the Francis turbine providing for higher draining efficiency at lower levels of stored energy compared to PAT, this difference is small but present 3.5. The model has been created in such a way that the user will be asked whether to use PAT or Francis turbine at the beginning of the simulation. This has been done as the problem owner wished for clear and easy evaluation of performance of different types turbines. Reason to believe that Francis turbines would yield much higher efficiency followed from Section 3.2. However, it is proven that, in this particular application of the OG, *i.e.* on 40 m of depth, pressure differences caused by the fluid column above the OB result in an acceptable range of flow-rates and consequently efficiency for both PAT as Francis turbines.

The result from several simulations of the set-up with single OB and generator (1S1G) of the MPC is that revenues from the standalone turbine turn out to be little higher compared to using a PAT. This also holds for longer simulations: a 30 day simulation shows that the percentual revenues are approximately 0.89% higher with standalone turbines. Standalone turbines generate 1.0% higher than a set-up without storage whilst PATs generate 0.12% higher revenues. This simulation of 30 days corresponds to 1440 time-steps with sampling time 30 minutes, this is the horizontal axis of the plots in Figure 4.1, 4.2, 4.3 and 4.4. In the fist three plots, the amount of energy stored, ES in megawatt-hour, is on the vertical axis. The vertical axis for the fourth plot, of the price data, corresponds to the energy price in Euro per megawatt-hour. Apart from the PAT and Francis simulation, an additional plot has been provided in Figure 4.3, to show the storing behaviour of the old model assuming use of PAT with η_T of 80%. A Francis turbine shows higher efficiency, more storage utilisation and higher revenues compared to the old model's storing behaviour.

Storage utilisation of the single OB set-up, with maximum storage of 2.4 MW h, with Francis turbine was higher than PAT. The actual storage and corresponding revenues have been provided in Table 4.1.

4.1.2 Up-scaled OB network

The problem owner and mr. Prins, *i.e.* stakeholders who represent the company, have shown interest in the effect of this varying efficiency in a network of connected OBs. A set-up is selected with 4 OBs and 2 generators (4S2G), in order to investigate the effect of varying

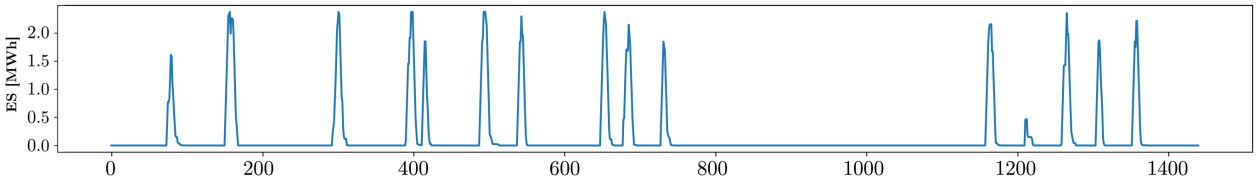

Figure 4.1 Storing improved MPC single set-up with PAT

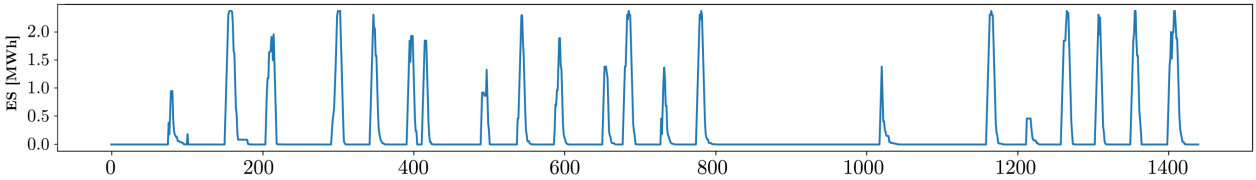

Figure 4.2 Storing improved MPC single set-up with Francis turbine

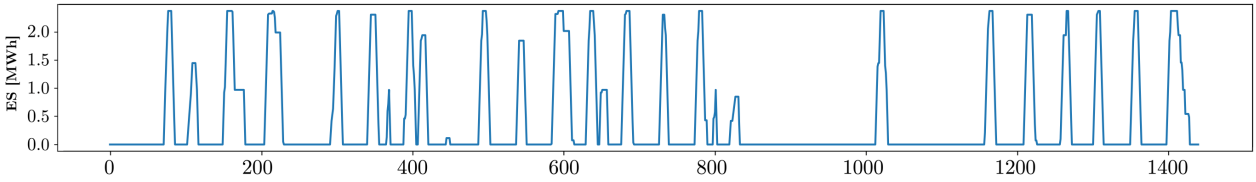

Figure 4.3 Storing old MPC single set-up with constant $\eta_T = 80\%$

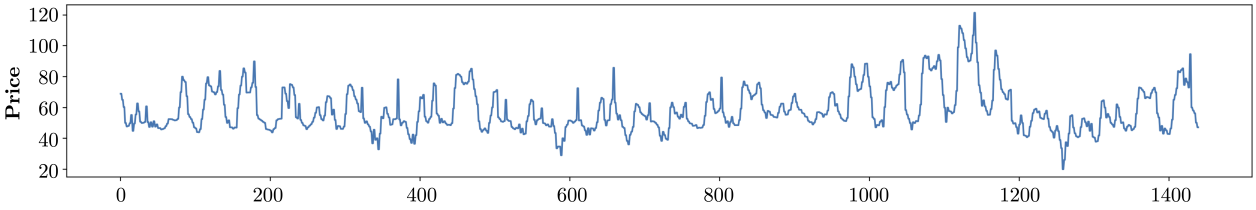

Figure 4.4 Day-ahead price data of one moth

efficiency in an up-scaled network. The set-up of the original model and the improved model are the same: the OBs have been connected like a square without diagonals, 2 of the OBs on an opposite corner of this square have been connected to a generator, energy can be transferred "for free" between OBs due to underwater cabling to spread stored energy. In the results obtained one comparison has been made: between the old model assuming $\eta_T = 0.80$

Model	**Turbine type**	**ES** in MWh	**Revenues** in €
Improved	PAT	33.7	110,912.76
	Francis	43.2	111,896.61
Old	$\eta_T = 0.80$	58.5	111,347.03
–	–	0.00	110,777.57

Table 4.1 Total energy stored (ES) and revenues for one month of simulation (1S1G)

and the improved model with the varying η_T caused by the use of Francis turbine. In the 1S1G set-up, more revenues are captured with less storage. However, with the increase of total capacity, significantly more energy will be stored in the set-up where constant efficiency is assumed generating higher revenues compared to using Francis turbine incorporating the varying η_T; the capacity outweighs the amount of storage. The results of one month of simulation have been depicted in Table 4.2, Figure 4.5 and 4.6 for the improved MPC with Francis turbine and the old model.

Model	**Turbine type**	**ES** in MWh	**Revenues** in €
Improved	Francis	135	186,034.40
Old	$\eta_T = 0.80$	200	187,791.10

Table 4.2 Total energy stored (ES) and revenues for one month of simulation (4S2G)

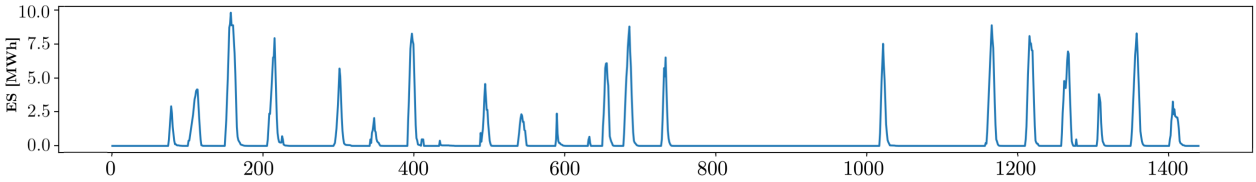

Figure 4.5 One month storage improved MPC with Francis turbine (4S2G)

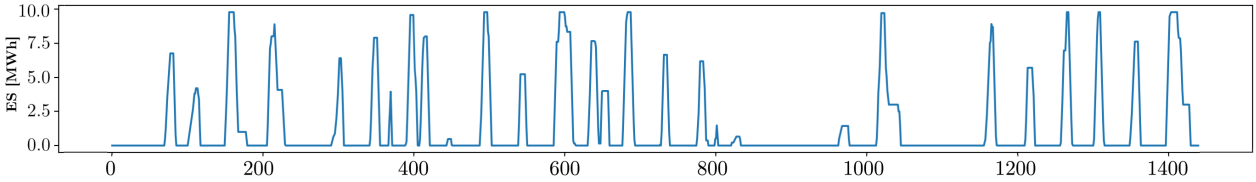

Figure 4.6 One month storage old MPC with $\eta_T = 80\%$ (4S2G)

4.2 Validation of results

The functions as expected. When energy is stored, at each iteration the predicted as well as the actual $E_{out,r}$ is calculated. The actual value is printed at each iteration as well as the η_T. These values are updated in accordance with the amounts of energy which is sent to the OBs. Furthermore, η_T influences the generated revenues: the current energy price multiplied with control variable for draining, the amount of stored energy and η_T yields the revenues for the battery system at that particular instance.

In order to put the the improved model to a test, the price data-set is altered. High price differences every one are introduced in the price data-set every once in a while, in the form

of sudden price drops and increases. It is expected and proven that significant amounts of energy will be stored when there are higher price differences present in the energy price data-set.

Previous research (Venturini et al., 2018) claims that Equation 3.1 deals with volumetric efficiency (Lyons, Plisga, and Lorenz, 2016), whilst Van Kessel claims that this has not been taken into account. Due to the fact that the literature and the mathematics match with his research, it is presumed that this has been dealt with provided the mathematics from Subsection 3.1.2.

4.3 Discussion

Turbine set-ups which incorporate varying efficiencies show more steep and spiky storage behaviour, depicted in Figure 4.1 and 4.2 for PAT and standalone turbine respectively, compared to storage behaviour assuming constant efficiency Figure 4.3. This spiky behaviour can easily be explained and points in the direction of valid and accurate model improvement. Due to the fact that efficiency will decrease as the amount of energy decreases, draining decisions will be carried out more radically in the higher range of turbine efficiency to grasp the most revenues from one draining decision. Revenues turn out higher in the cases where constant efficiency is assumed, as there is equal efficiency over the entire range of stored energy.

Revenues of instances where storage is utilised will always turn out higher than those where it is not as depicted in Table 4.1, this pledges in favor of the improved model's validity, *i.e.* the accuracy of the measurement or in this case passing multiple sensitivity analyses and generating more convincing simulation results, and its reliability, *i.e.* consistency in generating similar results in similar conditions. When storage is drained, the efficiency will drop with it and provided the figures in Subsection 4.1.1, the OBs are drained rather quickly, to a zero-level indirectly. It is observed that storage will in some cases first drop to the amount of energy where the lower efficiency bound is below zero, *e.g.* in Figure 4.1 around 100, 300, 500, between 600 and 800 and at 1200 seconds and in Figure 4.2 around 100, 200, 400, between 600 and 800 and all instances above 1000 seconds.

Provided the preceding paragraph, the improved MPC thus shows that it accounts for the zero-efficiency range, *i.e.* for the revenue loss in the draining operations. Hence, the revenue maximisation process functions optimally and the storage is used optimally. The resulting

revenues depicted in Table 4.1 are an average of three simulations of the same data-set. It is concluded that model produces consistent output in several simulations. Also it is proven that revenues turn out little lower provided the implementation of varying η_T, compared to a case where a constant and comparable efficiency is assumed. Note that the previously stated on the case where no energy will be stored only holds when the system is able to sell its energy at all times.

Chapter Five

Conclusions

This study set out to investigate the effect of including efficiency losses caused by using a PAT on the revenue optimisation process. Analysis of the current model has proven that including more realistic values for the efficiency will cause the model to reduce storing operations to a minimum. In the following paragraphs, the sub-questions will be answered sequentially.

The first sub-question has been treated in Chapter 2: in order to investigate the effect of efficiency on storing and draining decisions validation by means of sensitivity analysis was done to understand which efficiencies cause the model to stop draining. Interesting is that the threshold for η_T proved higher in both the direct and indirect model compared to the single set-up: around 86% and 50% for the connected and single set-up respectively. The lower threshold for storage in the single set-up allowed for the investigation on varying and consequently lower efficiencies for PAT and standalone turbines.

The model has been generalised for the use of larger networks, it is to receive as an input the exact layout of the offshore system, among which are the number of OBs in a cluster, the number of clusters, the adjacency matrix (of how all batteries are connected), *etc.* Analysis on the increase in revenues has been proven and confirmed once again for both the direct and indirect model, energy storage has proven to lead to higher revenues in all of the investigated set-ups, complying with the second sub-question.

The third sub-question has been treated in Section 3.2, concluding from it is that the efficiency depends on the height of the column above the storage causing pressure difference. This column height has been converted into the (relative) amount of stored energy and allows for a realistic energy-varying efficiency. These variables have been linked through curve fitting of data on draining flow-rates obtained from Van Kessel, 2020.

Based on feasible regulations for turbines operating in a head range similar to the on which the OG is subject to, an estimate of the start-up time of the turbine has been made. It is assumed that there will be a full power loss for the first two seconds of draining. Provided a sampling time of 1800 s, this is considered negligible.

Complying with the fifth sub-question, revenues with using a standalone turbine or PAT will differ slightly, around 0.89% increase for using standalone turbine. An important observation is that using a standalone turbine, with higher efficiency on smaller values of stored energy, energy will be stored more often. The additional storing peaks in Figure 4.2, compared to storage with PAT as depicted in Figure 4.1, are somewhat lower meaning that then less energy is stored. In those cases however, is the standalone turbine able to generate additional revenues due to the higher efficiency at lower amounts of stored energy.

Answering the sixth sub-question after researching the single set-up has luckily proven rather intuitive. The direct model shows similar behaviour to the single set-up: the major differences are that the overall capacity is increased largely and additionally, not all batteries are connected to the grid, and thus cannot sell their energy: yielding small storage differences in the network of connected OBs. The old model with constant η_T stores more energy, and more often, additionally generates lower revenues compared to using Francis turbine incorporating the varying η_T, in the 1S1G set-up. With the increase of storage capacity, in the 4S2G set-up, again more energy will be stored more often and the revenues will be higher as well. The indirect model shows that the batteries which can only be utilised via discharge of other batteries will not be used, which is conform hypothesis: there are simply too many losses involved when utilising those batteries.

5.1 Main conclusion

This research has shown that including efficiency loss due to the use of PAT decreases the storage utilisation and results in more spiky storing behaviour compared to using a constant value for η_T. These findings suggest that the revenue optimisation process functions optimally as the storage is intuitively utilised and revenues are maximised. The varying η_T of PAT and Francis turbines show comparable storing behaviour to a constant η_T of 80%, where revenues from using PAT turn out little lower and Francis little higher; as depicted in Figure 4.3, 4.1 and 4.2 respectively. It entails that the overall efficiency of PAT is little under 80% and that of Francis turbine little over 80%.

Additionally, Table 4.1 shows less storage is used with the implementation of a Francis turbine compared to an assumed constant η_T whilst revenues, in smaller set-ups, are higher! This entails that the **model manages to generate maximum revenues** from storage and **maximise draining efficiency**. This supports validation on the more spiky storing behaviour of a set-up containing a turbine with varying efficiency.

5.2 Limitations and recommendations

One aspect has been overlooked in Equation B.2. Namely, the time needed to drain the system might be smaller than the sampling time, $T_d < T_s$. If that was not considered, the flow-rate would have been assumed to be relatively small and constant over the sampling time yielding very low efficiency which is an inaccurate representation of reality. Thus before each draining decision, the following has to be checked; whether if the draining time is greater than or equal to the sampling time, then Equation B.2 is proposed to be used to estimate draining efficiency. The minimum draining time can be determined using the following expression

$$T_d = \frac{V_c}{Q_T}, \tag{5.1}$$

which is compared to the sampling time as follows $T_d \geq T_s$. Additionally, if the current stored volume is relatively small and sampling time greater than the draining time, it would wrongly yield small flow-rate and thus wrongly yield low efficiency, as the efficiency is low at small flow-rates.

Inertia might also play a role in the rotating turbine blades. After operation, the turbines will keep moving until friction, and the conversion of rotational energy to electricity, slows them down. Vice versa is force needed to make the blades rotate. Inertia has proven to be a useful parameter that can be used in calculations for reliable idea about dynamic behavior of the rotating unit (Piriz et al., 2012). This inertia might yield additional insight in the start-up process of turbines. However, no specific turbine dimensions have been proposed and in this stage of development of the OG, it is difficult to investigate this in detail.

Currently, an educated assumption for the the start-up time of turbines has been found. It is however not implemented in the model, as promoting the system to store after the efficiency penalty, the model. This could be investigated in more detail: by studying control of turbine governors. By controlling either the guide vanes (for standalone turbines) or simply the opening of the valve (for PATs), the power output can be optimised and the start-up time can be reduced. This optimal control leads to optimal frequency response of the blades,

which closely relate to the power output (Jain and Patel, 2014).

Average efficiency has been used as discussed in the validations section. However, this is not an exact estimation of the real-world dynamics, dynamical (efficiency) behaviour could be investigated in more detail using CFD. However, in accordance with stakeholder and first supervisor of this research, no CFD was involved in this research.

The peak capacity of sustainable energy sources, like windmills, connected to an OB network versus the peak capacity of energy connections between the OB and land, the energy grid has not been investigated in this research. This entails that if the peak capacity of windmills is higher than the peak capacity of the energy outflow from OB networks, energy will need to be stored. The potential of incorporating this limitation is that larger number of energy producing units (such as windmills) can be connected to OB networks.

The MPC has been complemented with a more realistic η_T and from Section 2.2, it has become clear that pumping efficiency can also greatly influence the storing behaviour. This has completely been disregarded throughout the research. The results were consistently obtained with constant a η_P of 95%. This is recommended to be part of future research, as the η_T also varies w.r.t. the fluid column above it, more power is needed to pump the fluid into the bladders with higher pressure on the system. This research may however serve as a basis for the methods on how to implement and investigate this varying η_P.

Currently, the OB systems can only operate in one state at a time. There are three possible states. The first state is where energy is stored, whilst this would not be likely in the case where a Francis turbine was implemented, as it will not be used as a pump as well.

The last two limitations both stem from the need of investigation on wear and maintenance of the OG. Cavitation, the process in where liquid vapour is formed due to a sudden pressure difference, is not included in the research. This is a common drawback of rotating structures and narrow parts in piping causing much wear. This will in its turn affect the performance of the pump and turbine system. It might be interesting for future investigation on maintenance and wear, which was not part of the scope of this research. Additionally, switching between pumping and PAT affects both the overall storage capacity/efficiency and greatly influences the life expectancy of the PAT (Gummer and Etter, 2008; Chirag Trivedi, Gandhi, and Michel, 2013). It might be better for the life expectancy of the PAT to let the bladders inflate to its maximum capacity before draining and accordingly minimising the number of switches (Chiragkumar Trivedi, 2013). Both the fact that this PAT setup is only able to go

through a certain number of cycles before breakdown and the effect that the startup time has on the flow-rate of the stored fluid have not been included in the scope of this research.

References

A. Carravetta S. Derakhshan Houreh, H. M. Ramos (2018). *Pumps as Turbines: Fundamentals and Applications*. Springer, Cham, Switzerland.

Bansal, R. K. (2017). "Chapter 1, 5, 6, 7, 10, 11". In: *A Textbook of Fluid Mechanics and Hydraulic Machines*. Ed. by R. K. Bansal. Laxmi Publications. ISBN: 9788131808153.

Breeze, Paul (2018). "Chapter 2 - Pumped Storage Hydropower". In: *Power System Energy Storage Technologies*. Ed. by Paul Breeze. Academic Press, pp. 13–22. ISBN: 978-0-12-812902-9. DOI: https://doi.org/10.1016/B978-0-12-812902-9.00002-X. URL: http://www.sciencedirect.com/science/article/pii/B978012812902900002X.

Casartelli, E et al. (Mar. 2019). "CFD simulation of transient startup for a low specific-speed pump-turbine". In: *IOP Conference Series: Earth and Environmental Science* 240, p. 082007. DOI: 10.1088/1755-1315/240/8/082007. URL: https://doi.org/10.10882F1755-13152F2402F82F082007.

Delgado, J. et al. (2019). "Variable speed operation of centrifugal pumps running as turbines. Experimental investigation". In: *Renewable Energy* 142, pp. 437–450. ISSN: 0960-1481. DOI: https://doi.org/10.1016/j.renene.2019.04.067. URL: http://www.sciencedirect.com/science/article/pii/S0960148119305518.

Derakhshan, Shahram and Ahmad Nourbakhsh (2008). "Experimental study of characteristic curves of centrifugal pumps working as turbines in different specific speeds". In: *Experimental Thermal and Fluid Science* 32.3, pp. 800–807. ISSN: 0894-1777. DOI: https://doi.org/10.1016/j.expthermflusci.2007.10.004. URL: http://www.sciencedirect.com/science/article/pii/S0894177707001367.

Dijkstra, Tom (2016). "Maximizing revenue of electricity generated by the Ocean Grazer. Implementation of a model predictive control on the storage reservoir of the Ocean Grazer." In: *Master thesis*. University of Groningen, Groningen.

Gummer, John and S. Etter (Jan. 2008). "Cracking of Francis runners during transient operation". In: 15, pp. 81–85.

Guo, Wencheng and Jiandong Yang (2018). "Modeling and dynamic response control for primary frequency regulation of hydro-turbine governing system with surge tank". In: *Renewable Energy* 121, pp. 173–187. ISSN: 0960-1481. DOI: https://doi.org/10.1016/

j.renene.2018.01.022. URL: http://www.sciencedirect.com/science/article/pii/S0960148118300223.

Jain, Sanjay V. and Rajesh N. Patel (2014). "Investigations on pump running in turbine mode: A review of the state-of-the-art". In: *Renewable and Sustainable Energy Reviews* 30, pp. 841–868. ISSN: 1364-0321. DOI: https://doi.org/10.1016/j.rser.2013.11.030. URL: http://www.sciencedirect.com/science/article/pii/S136403211300779X.

Kalogeri, Christina et al. (2017). "Assessing the European offshore wind and wave energy resource for combined exploitation". In: *Renewable Energy* 101, pp. 244–264. ISSN: 0960-1481. DOI: https://doi.org/10.1016/j.renene.2016.08.010. URL: http://www.sciencedirect.com/science/article/pii/S096014811630711X.

Lira, A et al. (2016). "Uncertainties in the estimate of wind energy production". In: Proceedings of the Energy Economics Iberian Conference–EEIC, Lisboa, Portugal, pp. 4–5.

"Chapter 3 - Auxiliary Equipment" (2016). In: *Standard Handbook of Petroleum and Natural Gas Engineering (Third Edition)*. Ed. by William C. Lyons, Gary J. Plisga, and Michael D. Lorenz. Third Edition. Boston: Gulf Professional Publishing, pp. 3-1 - 3–66. ISBN: 978-0-12-383846-9. DOI: https://doi.org/10.1016/B978-0-12-383846-9.00003-5. URL: http://www.sciencedirect.com/science/article/pii/B9780123838469000035.

NextKraftwerke (2020). *Balanceringsenergie Next Kraftwerke*. URL: https://www.next-kraftwerke.nl/kennis/balanceringsenergie (visited on 04/10/2020).

Nicolle, J, A M Giroux, and J F Morissette (Mar. 2014). "CFD configurations for hydraulic turbine startup". In: *IOP Conference Series: Earth and Environmental Science* 22.3, p. 032021. DOI: 10.1088/1755-1315/22/3/032021. URL: https://doi.org/10.1088%2F1755-1315%2F22%2F3%2F032021.

Niekolaas, Kirsten (2020). "Revenue maximization of distributed Ocean Battery systems through Model Predictive Control." In: *Master thesis*. University of Groningen, Groningen.

Onwubolu, Godfrey C. (2005). "Chapter 7 - Data acquisition". In: *Mechatronics*. Ed. by Godfrey C. Onwubolu. Oxford: Butterworth-Heinemann, pp. 257–278. ISBN: 978-0-7506-6379-3. DOI: https://doi.org/10.1016/B978-075066379-3/50008-2. URL: http://www.sciencedirect.com/science/article/pii/B9780750663793500082.

Overheid (2020). *Artikel 10.39 Netcode elektriciteit Wetten Overheid*. URL: https://wetten.overheid.nl/jci1.3:c:BWBR0037940&hoofdstuk=10&paragraaf=10.8&artikel=10.39&z=2020-04-04&g=2020-04-04 (visited on 04/10/2020).

Pelc, Robin and Rod M. Fujita (2002). "Renewable energy from the ocean". In: *Marine Policy* 26.6, pp. 471–479. ISSN: 0308-597X. DOI: https://doi.org/10.1016/S0308-597X(02)00045-3. URL: http://www.sciencedirect.com/science/article/pii/S0308597X02000453.

Piriz, Héctor et al. (Jan. 2012). "Inertia of hydro generators. Influence on the dimensioning, cost, efficiency and performance of the units". In:

Qin, Chao, Gordon Saunders, and Eric Loth (2017). "Offshore wind energy storage concept for cost-of-rated-power savings". In: *Applied Energy* 201, pp. 148–157. ISSN: 0306-2619. DOI: https://doi.org/10.1016/j.apenergy.2017.04.077. URL: http://www.sciencedirect.com/science/article/pii/S0306261917304683.

Ramos, H. and A. Borga (1999). "Pumps as turbines: an unconventional solution to energy production". In: *Urban Water* 1.3, pp. 261–263. ISSN: 1462-0758. DOI: https://doi.org/10.1016/S1462-0758(00)00016-9. URL: http://www.sciencedirect.com/science/article/pii/S1462075800000169.

Simske, Steven (2019). "Chapter 5 - Sensitivity analysis and big system engineering". In: *Meta-Analytics*. Ed. by Steven Simske. Morgan Kaufmann, pp. 187–201. ISBN: 978-0-12-814623-1. DOI: https://doi.org/10.1016/B978-0-12-814623-1.00005-8. URL: http://www.sciencedirect.com/science/article/pii/B9780128146231000058.

Steller, Janusz et al. (June 2008). "Pumps as turbines for hydraulic energy recovery and small hydropower purposes in Poland". In: pp. 2–3.

Trivedi, Chirag, Bhupendra Gandhi, and Cervantes J. Michel (2013). "Effect of transients on Francis turbine runner life: a review". In: *Journal of Hydraulic Research* 51.2, pp. 121–132. DOI: 10.1080/00221686.2012.732971. eprint: https://doi.org/10.1080/00221686.2012.732971. URL: https://doi.org/10.1080/00221686.2012.732971.

Trivedi, Chiragkumar (2013). *Transients in high head Francis turbines*.

Van Kessel, Thimo (2020). "Simulation of the energy flow of an offshore energy storage system." In: *Bachelor thesis*. University of Groningen, Groningen.

Vänskä, Vesa (2020). *Automatic frequency restoration reserve FINGRID OYJ*. URL: https://www.fingrid.fi/en/electricity-market/reserves_and_balancing/automatic-frequency-restoration-reserve/ (visited on 04/10/2020).

Venturini, Mauro et al. (2018). "Development of a physics-based model to predict the performance of pumps as turbines". In: *Applied Energy* 231, pp. 343–354. ISSN: 0306-2619. DOI: https://doi.org/10.1016/j.apenergy.2018.09.054. URL: http://www.sciencedirect.com/science/article/pii/S030626191831345X.

Verschuren, Piet, Hans Doorewaard, and Michelle Mellion (2010). *Designing a research project*. Vol. 2. Eleven International Publishing The Hague.

Wieringa, Roel J (2014). *Design science methodology for information systems and software engineering*. Springer.

Williams, Arthur et al. (2003). *Pumps as turbines: a user's guide*. ITDG Pub.

Yang, Weijia et al. (2016). "Response time for primary frequency control of hydroelectric generating unit". In: *International Journal of Electrical Power and Energy Systems* 74, pp. 16–24.

Zhao, Jie et al. (2018). "Improved nonlinear turbine-governor model and parameter assessment for a large hydropower plant". In: *International Transactions on Electrical Energy Systems* 28.5. e2525 ITEES-17-0179.R2, e2525. DOI: 10.1002/etep.2525. eprint: https://onlinelibrary.wiley.com/doi/pdf/10.1002/etep.2525. URL: https://onlinelibrary.wiley.com/doi/abs/10.1002/etep.2525.

APPENDICES

Appendix A

Complemented existing Matlab turbine model

In order to easily obtain useful parameters for this research, the Matlab turbine model from Van Kessel, 2020, is complemented and slightly changed. It has been converted into a function, which can be seen in the first line of Listing A.1. The outputs of this model are relative amount of stored energy w.r.t. E_{max}, relative average flow-rate w.r.t. $Q_{T,opt}$ and the average turbine efficiency η_T respectively. The input of the function is depth, `D=d`, replacing `D=40`, allowing for simulations of varying head, provided Equation 3.6. The lines of code added to the existing Matlab model, that is in line 1 and lines 58 to 71, have been depicted in Listing A.1.

Listing A.1 Complementary code in Matlab

```
1  function [Er, Qrel, AvgN]=roundtrip(d)


58 AvgN = mean(Nt)
59 % determine average value of turbine efficiency and store it in
       variable AvgN
60 AvgQ = mean(Qt)
61 % determine average value of turbine flow-rate and store it in
       variable AvgQ
62 Ek = Eout/3600;
63 % convert model outputs to usable outputs, i.e. J to MWh
64 Emax = 0.3475;
65 % maximum amount of energy in model, determined with max head
66 Er = Ek/Emax;
67 % relative amount of energy w.r.t. maximum drained energy
68 n=find(Nt == max(Nt(:)));
69 % find at which point efficiency is highest
70 Qoptimal = 4.993;
71 % determine optimal flow-rate is found by: Qoptimal = Qt(n), for max
       head of 40 m
72 Qrel = AvgQ/Qoptimal;
73 % relative of flow-rate w.r.t. optimal flow-rate
74 end
```

Appendix B

Stored energy and flow-rate

Replacing the power of Equation 3.7b with the supplied power obtained from Equation 3.1a, that is the bottom part of the fraction, a relationship between the current amount of stored energy and the static head can be obtained.

$$\begin{aligned} E_k &= \rho_f \cdot g \cdot H_s \cdot T_s \cdot Q_T \\ &= \rho_f \cdot g \cdot H_s \cdot T_s \cdot A_i \cdot v_f, \quad (3.3) \\ &= \rho_f \cdot g \cdot H_s \cdot T_s \cdot A_i \cdot \sqrt{\frac{2 \cdot g \cdot H_s}{1+K}}, \quad (3.2) \\ &= (\frac{\rho_f \cdot A_i \cdot T_s \cdot \sqrt{2 \cdot g^3}}{\sqrt{1+K}}) \cdot {H_s}^{1.5} \end{aligned} \tag{B.1}$$

This results in Equation B.2 for approximating the change in static head at the current energy storage level,

$$H_s = \left(\frac{E_k \cdot \sqrt{1+K}}{\rho_f \cdot A_i \cdot T_s \cdot \sqrt{2 \cdot g^3}} \right)^{\frac{2}{3}} \tag{B.2}$$

Now, there is an expression relating the stored energy level and corresponding head, which are the only variables in Equation B.2. Note that sampling time, T_s, is being treated as a constant here. This allows for estimation of the average flow-rate, provided the stored energy level at the beginning of each iteration. Given Equation 3.4, it is concluded that the average flow-rate will increase proportional to a third degree root of stored energy during drainage phase, i.e. $Q_T \propto \sqrt[3]{E_k}$. This proportionality can be verified by plotting the data and fitting a curve of a cube root to it, which will be covered in the following two sections.

B.1 Curve fitting for flow-rate

The script provided in Listing B.1 is used to obtain arrays storing $E_{out,r}$ and Q_T, to which the cubic root curve is fit. The script does iterative function calls to the Matlab turbine model, which is explained and complemented in Appendix A, in order to obtain the data points depicting flow-rate behaviour w.r.t. relative amount of stored energy. It has been depicted in Listing B.1. The goal is to prove the earlier stated, that $Q_T \propto \sqrt[3]{E_k}$. Therefore,

Listing B.1 Matlab script for obtaining data of relative energy versus flow-rate

```
4  Er=[]; Qrel=[];
5  % initialise empty vectors
6  d=9.0001;
7  % limiting value of Er and Qrel, where head approaches zero
8  [Er,Qrel]=roundtrip(d);
9  % roundtrip(d) is the Matlab model (Van Kessel, 2020), turned into a
       function expecting only the depth as an input
10 d=10; i=2;
11 % initialise d and i for while loop
12 while i<=15
13      [Er(i),Qrel(i)]=roundtrip(d);
14      Er=[Er,Er(i)]; % add element to vector Er
15      Qrel=[Qrel,Qrel(i)];
16      i=i+1;          % keeps iterating until i=15
17      d=d+2;          % increments of 2 meter
18 end
19 vectorQ=[Er;Qrel]'
20 % obtain data for curve fit
```

the function that is used to guess the behaviour therefore reads

$$y = a + b \cdot \sqrt[3]{x - c} \tag{B.3}$$

The arrays storing $E_{out,r}$ and Q_T are extracted from the Matlab model as described in Section 3.2. Note that the first simulation will be done with with maximum head, which is equal to the depth, such that the maximum energy from draining can be determined. The goal is to obtain a mathematical relation between the stored energy and flow-rate. Equation B.3 is the guessed, continuous curve. Now, provided that computers can not deal with analog, continuous functions, the data is to be sampled (Onwubolu, 2005). The `NumPy` library is used for computing the natural logarithm of x element-wise. The data to which the curve is fit is stored in arrays `x_data` and `y_data` as mentioned in Section 3.2. In order to actually fit the curve, the curve fitting package `curve_fit` from the `SciPy` optimisation library is used. The curve fit package determines the function which most closely matches the data by using least-squares minimisation. The line numbers correspond to the ones in the actual code, this provided code starts at line 33. In the preceding lines, the data has been collected and stored in arrays, which is not of interest when explaining the curve fit

Listing B.2 Curve fit for flow-rate in Python

```
import numpy as np
from scipy import optimize
def cbrt_func(x,a,b,c):
    return a+b*np.cbrt(abs(x-c)) #guess function called cbrt_func
init = [0.5, 0.4, 0.08] # guess values for a,b,c
params, fit = optimize.curve_fit(cbrt_func,x_data,y_data,p0=init)
print(params)
# params are the values of a,b,c which ensure best fit determined by
    the scipy optimize curve fit package
plt.scatter(x_data, y_data, label='Data')
# scatter plot of the data from the simulations in Matlab
plt.plot(x_data, ln_func(x_data, params[0], params[1], params[2]),
    label='Fitted function', color='cornflowerblue', linewidth=2)
# plot of the fitted curve in lighter blue, thickness of 2, the data
    values x_data have been plugged into the fitted curve
plt.legend(loc='best')
# adding a legend for the plot
plt.xlabel('Relative amount of stored energy (%)')
plt.ylabel('Turbine efficiency (%)')
# naming the x and y axis
plt.show() # displaying the plot
```

procedure. The output of this code will be a plot of the data points obtained from simulation of the Matlab model in blue and the fitted function, or curve, in a lighter shade of blue. This plot is provided in Figure B.1, and the optimal values of the parameters from Equation B.3 which are provided in Table B.1. All corresponding lines of code for the curve fitting are provided in Listing B.2.

a	b	c
53.32	8.485	8.419

Table B.1 Output parameters for flow-rate curve-fit of cubic root function

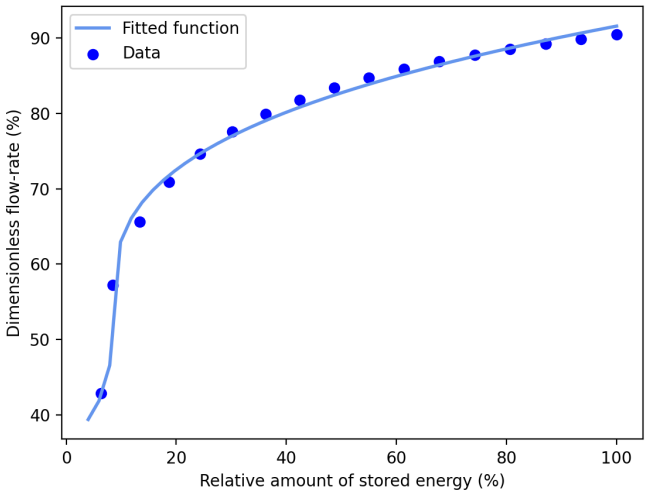

Figure B.1 Curve fit of average flow-rate corresponding to relative amount of stored energy

Appendix C

Stored energy and draining efficiency

The script provided in Listing B.1 is used to obtain arrays storing $E_{out,r}$ and η_T. The script does iterative function calls to the Matlab turbine model in order to obtain the data points depicting turbine efficiency behaviour w.r.t. relative amount of stored energy. The goal is to obtain a mathematical relation between the two. Now, provided that computers can not deal with analog, continuous functions, the data is to be sampled (Onwubolu, 2005). The `NumPy` library is used for computing the natural logarithm of x element-wise. The data to which the curve is fit is stored in arrays `x_data` and `y_data` as mentioned in Section 3.2. In order to actually fit the curve, the curve fitting package `curve_fit` from the `SciPy` optimisation library is used. The curve fit package determines the function which most closely matches the data by using least-squares minimisation. The line numbers correspond to the ones in the actual code, this provided code starts at line 50. In the preceding lines, the data has been collected and stored in arrays, which is not of interest when explaining the curve fit procedure. The output of this code will be a plot of the data points obtained from simulation of the Matlab model and the fitted functions, or curves. This plot is provided in Figure C.1. All corresponding lines of code for the curve fitting are provided in Listing C.2.

Listing C.1 Matlab script for obtaining data of relative energy versus efficiency

```
4  i=2;
5  Er=[]; AvgN=[];
6  d=9.0001;
7  [Er,Qrel,AvgN]=roundtrip(d);
8  d=10;
9  while i<=15
10      [Er(i),Qrel(i),AvgN(i)]=roundtrip(d);
11      Er=[Er,Er(i)];
12      AvgN=[AvgN,AvgN(i)];
13      i=i+1;
14      d=d+2;
15 end
16 vectorN=[Er;AvgN]'
```

C.1 Curve fitting for draining efficiency

The arrays storing $E_{out,r}$ and η_T are extracted from the Matlab model as described in Section 3.2. Note that the first simulation will be done with with maximum head, which is equal to the depth, such that the maximum energy from draining can be determined. Every subsequent simulation will be with lower values for head, increments of 1 m. The data output from Figure 3.2 seems to have both a vertical and horizontal asymptote. Therefore, it would be logic to fit a rational function to the data. However, this behaviour might as well be mimicked by either a power function, natural logarithm or exponential/logistic functions. Now, in order to obtain the best fit, all of the aforementioned curves will be fitted and measured for their accuracy, by means of the statistical measure R-squared. It is a measure between 0 and 1, which tells exactly what proportion of the data can be represented with the proposed curve. In some of the guessed curves, absolute values have been used, for example for the natural logarithm. This is done in order to prevent domain errors from occurring, since negative numbers are not in the domain of the natural logarithm. The negative numbers are not of concern in the actual model, because the efficiency will be zero below a 6.34 percent of maximal stored energy, which has become clear form the data. Hence, the implemented function will have no absolute values, it is only used for error-prevention purposes.

A plot of the optimal curve fit is provided in Figure C.1. The optimal function, Equation C.1, has been obtained by investigation on R-squared values as depicted in Table C.1. The optimal parameters of Equation C.1 have been provided in Table C.2.

Listing C.2 Curve fit for efficiency in Python

```
50 plt.scatter(x_data, y_data, label='Data', color='b') #plot data
51 import matplotlib.pyplot as plt
52 import numpy as np
53 from scipy import optimize
54
55 ## fitting a natural logarithm
56 def ln_func(x,d,e,f):
57     return d*np.log(abs(x-e))+f  #guess function called ln_func
58 init_guess_ln = [5,6,71] # guess values for a,b,c
59 params_ln, fit2 = optimize.curve_fit(ln_func,x_data,y_data,p0=
      init_guess_ln)
60 print('params_nl =',params_ln) # print curve fit parameters, i.e. are
      the values of a,b,c which ensure best fit determined by the scipy
      optimize curve fit package
61 y_ln = ln_func(x_data, params_ln[0], params_ln[1], params_ln[2]) # y
      coordinate of fitted function
62 plt.plot(x_data, y_ln, label='Natural logarithm', color='lightblue',
      linewidth=2) # plot function in lightblue, where data values x_data
       have been plugged into the fitted curve
63 absError_ln = y_ln - y_data # absolute error
64 SE_ln = np.square(absError_ln) # squared errors
65 Rsquared_ln = 1.0 - (np.var(absError_ln) / np.var(y_data)) #
      statistical performance measure, of how close the curve fit matches
       the data, a value between 0 and 1
66
67 ## fitting a power function
68 def p_func(x,k,l,m,n):
69     return k*((abs(x-l))**(-m))+n
70 init_guess_p=[-44,1,95]
71 params_p, fit4=optimize.curve_fit(p_func,x_data,y_data,p0=init_guess_p
      )
72 print('params_p  =',params_p)
73 y_p = p_func(x_data, params_p[0], params_p[1], params_p[2], params_p
      [3])
74 plt.plot(x_data, y_p, label='Power function', color='cornflowerblue',
      linewidth=2)
75 # performance R-squared
76 absError_p = y_p - y_data
```

```
77 SE_p = np.square(absError_p) # squared errors
78 Rsquared_p = 1.0 - (np.var(absError_p) / np.var(y_data))
79
80 ## fitting a rational function
81 def rational_func(x,a,b,c):
82     return -a/(abs(x-b))+c
83 init_guess_rational=[114,3,92]
84 params_rt, fit1=optimize.curve_fit(rational_func,x_data,y_data,p0=
       init_guess_rational)
85 print('params_rt =',params_rt)
86 y_rt = rational_func(x_data, params_rt[0], params_rt[1], params_rt[2])
87 plt.plot(x_data, y_rt, label='Rational function', color='darkblue',
       linewidth=2)
88 # performance R-squared
89 absError_rt = y_rt - y_data
90 SE_rt = np.square(absError_rt) # squared errors
91 Rsquared_rt = 1.0 - (np.var(absError_rt) / np.var(y_data))
92
93 ## fitting an exponential/logistic function
94 def exp_func(x,g,h,i,j):
95     return -g*np.exp(-h*(x-i))+j
96 init_guess_exp=[ 1.56883326e+02,  1.48002531e-01, -5.30917909e+00,
       9.01132244e+01]
97 params_exp, fit3=optimize.curve_fit(exp_func,x_data,y_data,p0=
       init_guess_exp)
98 print('params_exp=',params_exp)
99 y_exp = exp_func(x_data, params_exp[0], params_exp[1], params_exp[2],
       params_exp[3])
100 plt.plot(x_data, y_exp, label='Exponential, logistic function', color
       ='black', linewidth=2)
101 # performance R-squared
102 absError_exp = y_exp - y_data
103 SE_exp = np.square(absError_exp) # squared errors
104 Rsquared_exp = 1.0 - (np.var(absError_exp) / np.var(y_data))
105
106 plt.legend(loc='best') # show legend of plotted curves at 'best'
       curves
107 plt.xlabel('Relative amount of stored energy (%)') # naming the x axis
108 plt.ylabel('Turbine efficiency (%)') # naming the y axis
```

```
109
110 print('\nFunction: ','R-squared value:')
111 print('RT         ',Rsquared_rt)
112 print('P          ',Rsquared_p)
113 print('EXP        ',Rsquared_exp)
114 print('LN         ',Rsquared_ln)
115 # print the performance measures of each curve fit
116 plt.show() # display the plot
```

Provided the result of the R-squared statistic in Table C.1, the power function proves to be the best fitting curve in this domain. It reads

$$y = k \cdot |x - l|^{-m} + n \tag{C.1}$$

where the optimal values of the parameters from this function have are provided in Table C.2.

Function	**R-squared value**
Rational function	0.9954
Power function	0.9984
Exponential function	0.9670
Natural logarithm	0.9785

Table C.1 Statistical performance measures (R-squared) for the fitted curves

k	l	m	n
-42.66	5.038	0.5225	95.46

Table C.2 Output parameters for efficiency curve-fit of the power function

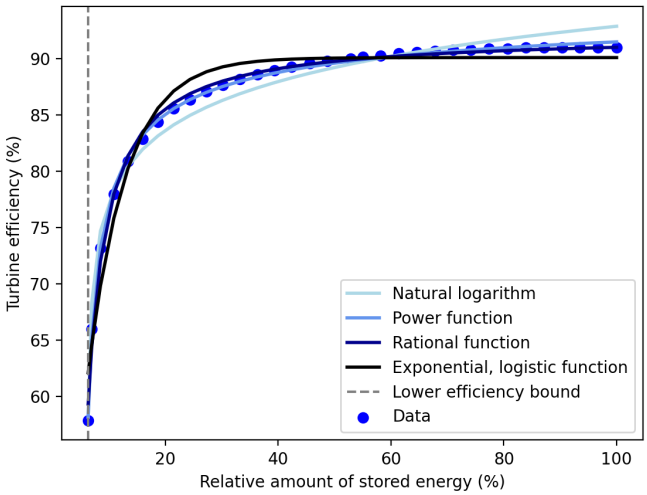

Figure C.1 Curve fit of efficiency corresponding to relative amount of stored energy

Appendix D

Implementation of the research findings

In this last appendix, the added lines of coding to the existing Python model have been provided, Listing D.1. The relevant findings of this research on PAT efficiency behaviour have been implemented, providing a newly complemented, more validated and robust MPC on the revenue optimisation process of the OG.

Listing D.1 Complemented coding in Python model

```
23 def type_turbine():
24     while True:
25         try:
26             Testinput = int(input("What type of turbine will be used?
                   Type 1 for PAT or 2 for standalone FRANCIS turbine: "))
                    # let user choose between standalone turbine (Francis)
                    and PAT
27         except ValueError:
28             print("Input is no integer")
29         if Testinput != 1 and Testinput != 2:
30             print("Input is not 1 or 2")
31             continue
32         else:
33             break
34     return Testinput
35 Testinput = type_turbine() # call function for user input

57 Eta_turbine = np.zeros((S,N)) # turbine efficiency
58 E_r = np.zeros((S,N)) # predicted relative energy
59 E_rel = np.zeros((S,N)) # actual relative energy
60 # initialise efficiency and relative energy vectors, for each battery
      (S) and timestep (N)
61 if Testinput == 1:
62     def turbine_eta(ER): # for PAT
63         if ER <= 0.0634:
64             return 0
```

```
65          else:
66              return (-42.66274921*(((100*ER)-5.03838764)**(-0.52251586)
                    )+95.45944474)/100
67
68  elif Testinput == 2:
69      def turbine_eta(ER): # for FRANCIS turbine
70          if ER <= 0.0634:
71              return 0
72          else:
73              return (-29.31567276*(((100*ER)-5.71879217)**(-0.99156659)
                    )+91.66293922)/100
74  # efficiency function functions for PAT and Francis turbines
        respectively

164 # calculate updated PREDICTED storage levels
165 for j in range(S):
166     es_hat[j,k] = es_hat[j,k-1] + Eta_pump*np.sum(u_form[S*dim+j:(S+G)
            *dim+j:dim]*ESav_hat[S:S+G,k]) - np.sum(u_form[j*dim+dim-1]*
            ESav_hat[j,k])
167 # calculate revenue
168 for j in range(S): # revenue from storages
169     E_r[j,k] = es_hat[j,k]/(E_max)
170     Eta_turbine[j,k] = turbine_eta(E_r[j,k])
171     R_hat[j,k] = -M_hat[k]*u_form[j*dim+dim-1]*Eta_turbine[j,k]*es_hat
            [j,k-1]

303 for j in range(S):
304     if i > 0:
305         E_rel[j,i] = ES[j,i]/(E_max)
306         if E_rel[j,i] <= 1:
307             Eta_turbine[j,i] = turbine_eta(E_rel[j,i])
308         else:
309             print('Exceeded storage')
310         R[j,i] = M[i]*u[j*dim+dim-1]*Eta_turbine[j,i]*ES[j,i-1]
311         print(f'Relative amount of stored energy = {E_rel[:,i]}')
312         print(f'Turbine efficiency = {Eta_turbine[:,i]}')

345 if Testinput == 1: a = "PAT has been used in simulation"
346 elif Testinput == 2: a = "FRANCIS turbine has been used in simulation"
347 print(a) # print the type of turbine used
```